Desalination and Water Treatment
www.deswater.com
1944-3994/1944-3986 © 2012 Desalination Publications. All rights reserved
doi: 10/5004/dwt.2012.3195

Taylor & Francis
Taylor & Francis Group

45 (2012) 100–111
July

Optimization of acetaminophen degradation by fluidized-bed Fenton process

Rowena Mañez Briones[a], Mark Daniel Garrido de Luna[a,b], Ming-Chun Lu[c,*]

[a]*Environmental Engineering Graduate Program, University of the Philippines, 1101 Diliman, Quezon City, Philippines*
[b]*Department of Chemical Engineering, University of the Philippines, 1101 Diliman, Quezon City, Philippines*
[c]*Department of Environmental Resources Management, Chia Nan University of Pharmacy and Science, Rende District, Tainan 71710, Taiwan*
Tel. +886 6 2660489; Fax: +886 6 2663411; email: mmclu@mail.chna.edu.tw

Received 11 August 2011; Accepted 2 November 2011

ABSTRACT

Recalcitrant compounds in pharmaceutical wastewaters render biological treatment inadequate. Conventional Fenton technology, though a promising alternative, suffers from high sludge generation. In this study, fluidized-bed (FB) Fenton process, an improvement of traditional Fenton method, was used to decompose acetaminophen (ACT) from aqueous solutions. Optimization of important parameters: initial pH, ferrous ion and hydrogen peroxide dosages, was carried out using Box–Behnken Design (BBD). Effects of all factors and their interactions on ACT decomposition were significant. At optimum operating conditions, ACT degradation reached 97.8% while iron removal of 62.92% was achieved. In addition, the high hydrogen peroxide efficiencies of FB-Fenton process with respect to ACT degradation and COD removal make this technology a cost-effective option in treating acetaminophen-contaminated wastewaters.

Keywords: Fluidized-bed Fenton process; Acetaminophen; Wastewater treatment; Box-Behnken design; Optimization; Advanced oxidation process

1. Introduction

Henry J. Fenton discovered the Fenton process in 1894 when he observed the oxidation of tartaric acid in the presence of ferrous ions and hydrogen peroxide. However, the application of this technology as a chemical oxidation process on an industrial scale was not exploited until the late 1960s [1]. Since then, modifications of Fenton technology were carried out primarily to reduce if not eliminate sludge production inherent in the process. Through the years, Fenton-based processes were proven effective in treating wastewaters of industries such as textile [2], alcohol production or distilleries [3], sugar [4], pesticides [5], insecticides [6], dyestuffs [7], explosives [8] and pharmaceuticals [9].

*Corresponding author.

Hydrogen peroxide, H_2O_2, is a weak oxidant with $E = 1.763$ V (SHE)$^{-1}$ and $E = 0.88$ V (SHE)$^{-1}$ in acidic and basic media, respectively [10]. If combined with ferrous ion (Fe^{2+}) catalysts, fast production of hydroxyl radicals (•OH) occurs [Eq. (1)]. Hydroxyl radical is a very powerful oxidizing agent with $E = 2.80$ V (SHE)$^{-1}$ [11]:

$$H_2O_2 + Fe^{2+} \rightarrow \bullet OH + OH^- + Fe^{3+} \quad k = 53 - 76 M^{-1}s^{-1} \tag{1}$$

The ferric ions (Fe^{3+}) produced also react with H_2O_2 to form a weaker radical, hydroperoxyl ion (•OH_2), with $E = 1.65$ V (SHE)$^{-1}$ [Eq. (2)] and in the process regenerate ferrous ion catalyst [11]:

$$H_2O_2 + Fe^{3+} \rightarrow \bullet OH_2 + Fe^{2+} + H^+ \quad k = 0.01\, M^{-1}s^{-1} \tag{2}$$

Values of rate constants suggest that ferric ions are produced more rapidly [Eq. (1)] than they are reduced to Fe^{2+} [Eq. (2)] resulting in the formation of excess Fe^{3+}at the end of the reaction. Neutralization of the final solution leads to the formation and accumulation of $Fe(OH)_3$ sludge. Additional cost for sludge handling and disposal remains the major drawback in using traditional Fenton technology for wastewater treatment [12].

Fluidized-bed Fenton was developed to minimize sludge production in conventional Fenton process. The generated ferric ions coat the surface of the carrier material and form iron oxides crystals [13]. Similar to the Fenton process, ferrous ions act as catalysts to produce hydroxyl radicals in solution. Aside from this homogenous reaction, heterogeneous chemical reaction occurs as iron oxide-coated carriers catalyze the generation of additional •OH for pollutant decomposition in solution [13]. Another advantage of FB-Fenton process is the quality of sludge produced. Ferric hydrolysis products in traditional Fenton process are puffy [14] and still contain 80% moisture even after dewatering. On the other hand, the sludge produced using FB-Fenton technology contains almost no water after drying [15] thereby reducing the cost required for sludge moisture removal. FB-Fenton is usually employed as a post-treatment process to remove recalcitrant compounds with low COD content (<1000 mg l^{-1}) [16]. A summary of advanced oxidation processes published on acetaminophen (ACT) degradation is presented in Table 1 [17–23].

In this study, Box–Behnken design (BBD) was used to optimize Fenton oxidation of ACT using a fluidized-bed reactor. Optimization of operating conditions was done with the aid of Design-Expert 7.0 software (Stat-Ease, Inc., Minneapolis, USA). ACT is one of the most commonly detected pharmaceutical in surface and wastewaters [24]. Hence, ACT was used as a target pollutant. Aside from optimization, this study also focused on the performance of FB-Fenton process in comparison to the traditional Fenton process.

2. Materials and methods

2.1. Chemicals and analytical methods

All chemicals used, including 35% H_2O_2, 99% 4-hydroxy acetanilide (ACT), $FeSO_4•7H_2O$, $HClO_4$, HNO_3, H_2SO_4, HCl, glacial acetic acid, $NH_4C_2H_3O_2$, $C_{12}H_8N_2•H_2O$, H_3PO_4, K_2TiO_4, acetonitrile, NaOH, $K_2Cr_2O_7$ and $Fe(NH_4)_2SO_4•6H_2O$ were purchased from Merck. All solutions were prepared using Millipore system deionized water with a resistivity of 18.2 MΩ.

Residual H_2O_2 in solution was analyzed following the titanium oxalate method and using ThermoSpectronic Genesys 20 spectrophotometer at 400 nm. ACT concentration was quantified by SpectraSYSTEM SN4000 HPLC equipped with Asahipak ODP-50 6Dand having its detector set at 220 nm. A mixture of 20 mmol l^{-1} phosphoric acid and acetonitrile (85:15) at 1 ml min^{-1} comprised the HPLC mobile phase. Total iron concentration in solution was computed through Perkin Elmer Analyst 200 AAS while surface area and composition of SiO_2 carriers were evaluated using N2-BET meter (Micromeritics) and SEM/EDS (EDAX), respectively. COD of the quenched samples were measured using closed reflux

Table 1
Summary of treatment technologies used in acetaminophen removal

Treatment technology	Operating conditions	Efficiency	Reference
H_2O_2/UV	Low pressure lamp = 254 nm C_O = 0.01 mM $C_{H_2O_2}$ = 20 mM pH = 5.5 time = 1 min T = 25°C	95% removal	[17]
Electro-oxidation	Anode = boron-doped diamond (BDD) Cathode = graphite C_O = 1.04 mM (100 mgl^{-1} TOC) time = 240 min Current = 450 mA Electrolyte = 0.05 mM Na_2SO_4 pH = 3.0 T = 35°C	98% mineralization	[18]

Continued

Table 1. *Continued*

Treatment technology	Operating conditions	Efficiency	Reference
UV-C/TiO_2 photocatalysis	Low pressure lamp = 15 W, 254 nm $C_{catalyst}$ = 0.4 g l^{-1} C_O = 4 mM time = 315 min pH = 5.6	≈97% removal and 56% mineralization	[19]
UV/TiO_2 photocatalysis	Lamp = 250W, 365 nm C_O = 50 μM $C_{catalyst}$ = 1 g l^{-1} pH = 6.9 time = 100 min	95% removal	[20]
Photo-Fenton oxidation	Lamp = 15 W, 365 nm C_O = 0.1 mM (10 mg l^{-1} TOC) pH = 2.5 Fe^{3+} = 0.2 mM $C_{H_2O_2}$ = 5.0 mM time = 30 min	96% removal after 10 min, 77% mineralization after 30 min	[21]
Solar photo-Fenton	C_O = 0.1 mM (10 mg l^{-1} TOC) pH = 2.5 FeOx = 0.2 mM $C_{H_2O_2}$ = 2.0 mM time = 5 min	100% removal	[21]
Solar photoelectro-Fenton	Anode = platinum sheet Cathode = carbon-PTFE air-diffusion electrode C_O = 1.04 mM Electrolyte = 0.05 mM Na_2SO_4 Current = 5 A pH = 3 Fe^{2+} = 0.40 mM T = 35°C time = 120 min	100% removal 75 % mineralization	[22]
Photo-Fenton	C_O = 0.066 mM $C_{H_2O_2}$ = 0.29 mM $Q_{H_2O_2}$ = 50 ml h^{-1} pH = 2.5 Fe^{2+} = 0.036 mM T = 40°C time = 120 min	71.5% mineralization	[23]

Note: The given concentrations are all initial values. C_O = ACT concentration; SRT = solids retention time; C_{H2O2}= H_2O_2 concentration; $C_{catalyst}$= catalyst concentration; FeOx = potassium ferrioxalate; PTFE = polytetrafluoroethylene; Q_{H2O2}=H_2O_2 flowrate.

$$\%\ mineralization = \frac{TOC_0 - TOC}{TOC_0} \times 100$$ where TOC_O = initial TOC, TOC = TOC at time *t*.

$$\%\ removal = \frac{C_0 - C}{C_0} \times 100$$ where C = ACT concentration at time *t*.

titrimetric method based on standard methods (American Public Health Association). TOC was analyzed using LiquiTOC (Elementar).

2.2. Fluidized-bed reactor

The cylindrical glass reactor for all experiments had inlet, outlet and recirculating sections (Fig. 1). Auxiliary equipment included an online pH probe and a peristaltic pump (Iwaki MD-10-NL12) for recirculation and fluidization. Because of the addition of support and carrier material for FB-Fenton, the effective working volumes for FB-Fenton and conventional Fenton processes were 1.45 and 1.5 l, respectively. SiO_2 were used as carriers.

2.3. Fenton and FB-fenton experiments

For FB-Fenton experiments, synthetic ACT wastewater at 5 mmol l^{-1} was poured into the reactor. The desired amount of $FeSO_4 \bullet H_2O$ was introduced into the solution. Glass beads of diameters 4 mm then 2 mm were carefully placed in the reactor to a depth of 3.5 and 1.25 cm, respectively, as support followed by 100 g SiO_2 carriers with average diameter of 0.5 mm. The pump was started and flowrate was adjusted until the SiO_2 carriers reached twice its initial height. Initial pH was adjusted with either concentrated $HClO_4$ or 0.1 mol l^{-1} NaOH. Finally, hydrogen peroxide solution was injected into the system to initiate Fenton reaction. Samples (4 ml) were taken from the top of the reactor at different time intervals of 0, 3, 5, 10, 20, 40, 60, 90 and 120 min. The samples were injected in amber bottles containing 4 ml 0.1 mol l^{-1} NaOH and 12 ml DI water. This procedure was done to stop the reaction. Prior to analysis, the quenched samples were filtered through a 0.2 μm syringe filter to remove iron precipitates. The same procedure as above was followed for conventional Fenton experiments except that glass beads and SiO_2 carriers were not added.

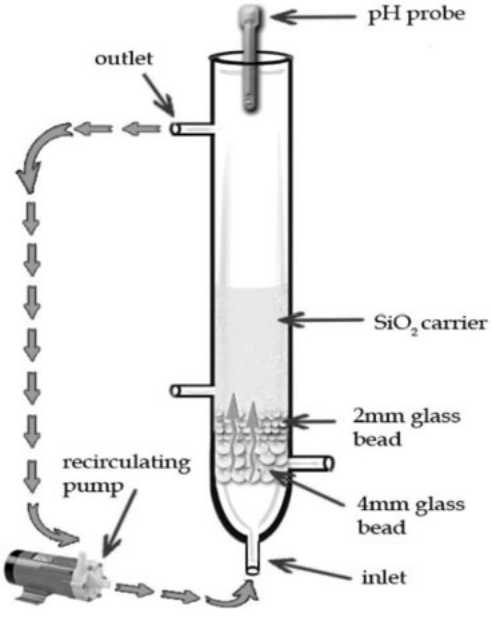

Fig. 1. Schematic diagram of reactor.

2.4. Box–Behnken design

BBD is a three-level design used to fit second-order models developed by Box and Behnken [25]. It is a spherical design with all points either on a sphere or at the center of the sphere. This design is used when there is only little interest in predicting responses at the extremes or corners of the cube – hence, the spherical design [26]. Furthermore, as convenience is required most of the time in experiments, the use of only a few levels for each factor is not really uncommon [25]. This design has the advantage of having very efficient number of required runs to fit the model. It can also be expanded to estimate the combinations of third order terms, that is, $x_1^2x_2$, $x_1^2x_3$ and $x_1x_2^2$ [27].

Design-Expert 7.0 (Stat-Ease, Inc., Minneapolis, USA) is a software for design of experiments (DOE). It includes combined, mixture, factorial and response surface designs. BBD is under response surface. This software guides the user all throughout the DOE and provides statistical analysis. First, details regarding categories (parameter), levels for each category, center points and responses are entered. Then, the software generates the runs required for the design. In this research, there were three parameters studied generating 17 runs with five replicates at the center point. In this table, results from actual experiments can be entered. Statistical analysis and optimization followed with the aid of the software.

3. Results and discussion

There were a total of 17 experimental runs with five replicates at the center point. The complete conditions and results for each run are shown in Table 2.

After 2 h of treatment, FB-Fenton process achieved the highest ACT degradation at pH 3 and maximum initial Fe^{2+} and H_2O_2 concentrations of 0.1 and 25 mmol l^{-1}, respectively. At these conditions, almost 98% of ACT was oxidized within 20 min of reaction time. In the other extreme, only 20.9% ACT decomposition was realized at pH = 2, $[Fe^{2+}]$ = 0.01 mmol l^{-1} and $[H_2O_2]$ = 15 mmol l^{-1} (Fig. 2).

Using Design-Expert 7.0 software (Stat-Ease, Inc., Minneapolis, USA), ACT decomposition best fit a reduced cubic model. For initial rates, full quadratic model was the most appropriate. Analysis of variance (ANOVA)

Table 2
Box-Behnken design experiment conditions and results at 5 mM ACT and 100 g SiO_2

Run	pH	Fe^{2+}, mM	H_2O_2, mM	ACT degradation, %	Initial rate, mM min^{-1}
1	3	0.100	25	99.2	0.840
2	4	0.010	15	77.0	0.208
3	3	0.010	5	54.6	0.061
4	2	0.100	15	87.5	0.194
5	3	0.055	15	91.2	0.213
6	3	0.100	5	57.2	0.414
7	4	0.100	15	92.8	1.241
8	3	0.055	15	93.2	0.182
9	2	0.055	5	57.7	0.028
10	3	0.010	25	79.7	0.090
11	2	0.055	25	85.4	0.193
12	3	0.055	15	94.1	0.188
13	4	0.055	25	98.0	0.560
14	3	0.055	15	93.4	0.210
15	4	0.055	5	57.70	0.426
16	3	0.055	15	93.1	0.285
17	2	0.010	15	20.9	0.148

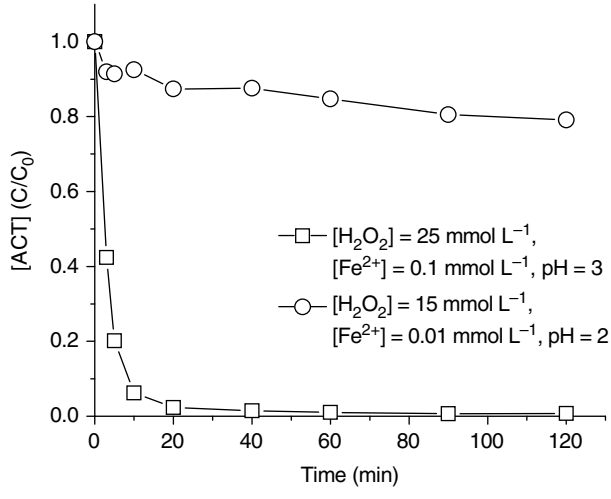

Fig. 2. ACT degradation profiles of selected FB-Fenton experiments.

for ACT degradation and initial rate are shown in Tables 3 and 4, respectively. All three operating parameters had significant effects on both responses.

Model equations for ACT degradation and initial rate in terms of dimensionless coded values (*A*, *B* and *C*), are given by Eqs. (3) and (4), respectively. *A*, *B*, and *C* in these equations correspond to variables X_1, X_2 and X_3 which denote actual values of initial pH, initial Fe^{2+} concentration and initial H_2O_2 concentration, respectively:

$$\%\text{ACT degradation} = 92.99 + 3.15A + 5.51B + 16.89C - 12.68AB + 3.17AC + 4.25BC - 10.72A^2 - 12.71B^2 - 7.57C^2 + 15.09A^2B + 12.21AB^2 \quad (3)$$

$$\text{Initial rate, mmol l}^{-1}\text{ min}^{-1} = 0.22 + 0.21A + 0.29B + 0.094C + 0.28AB - 0.0079AC + 0.099BC + 0.073A^2 + 0.12B^2 + 0.014C^2 \quad (4)$$

where

$$A = \frac{X_1 - 3}{1} \quad B = \frac{X_2 - 0.055}{0.045} \quad C = \frac{X_3 - 15}{10}$$

As shown in the Table 3, all the terms in the reduced cubic model are significant. This implies that the Eq. (3) cannot be simplified and all terms must be included. For the initial rate, insignificant terms are *AC* and C^2 (Table 4). These terms can be reduced in the equation to improve model. Also, these terms have the lowest numerical coefficient in Eq. (4), which means that increasing the values of the terms do not significantly affect the response.

In agreement with ANOVA results, the model equations show that all three parameters taken singly (*A*, *B* and *C*) have positive effects on ACT degradation. Hydrogen peroxide dosage, having the largest coefficient (16.89), exerts the greatest influence on ACT degradation. On the other hand, interaction effect (*AB*) and quadratic terms (A^2, B^2 and C^2) have negative coefficients indicating an inverse relationship on ACT degradation.

The high correlation between actual experimental data and the model for ACT degradation (R^2 = 0.999) and initial rate (R^2 = 0.990) are shown in Figs. 3 and 4, respectively. Actual data are ACT degradation results of experiments based from HPLC analysis of actual ACT concentration. Predicted values are ACT degradation values using the model equation [Eq. (3)] generated by the software.

3.1. Effect of operating parameters on ACT degradation and initial rate

ACT degradation in response to variations in operating parameters is shown in Fig. 5. The effect of pH on ACT degradation is more pronounced at low [Fe^{2+}] (0.01 mmol l^{-1}) [Fig. 5(a)]. At low pH (2) and medium [H_2O_2] (15 mmol l^{-1}), effect of increasing [Fe^{2+}] (from 0.01 to 0.1 mmol l^{-1}) is very evident [Fig. 5(b)] as ACT degradation increased from 20.9% to 87.5%. A low pH, which indicates higher [H^+] in solution, inhibits the regeneration

Table 3
ANOVA for ACT degradation

Source	Sum of squares	df	Mean square	*F*-value	*p*-value	
Model	7402.654	11	672.9686	702.3064	<0.0001	significant
A-pH	39.73652	1	39.73652	41.46882	0.0013	significant
B-Fe^{2+}	121.5957	1	121.5957	126.8966	<0.0001	significant
C-H_2O_2	2281.111	1	2281.111	2380.555	<0.0001	significant
AB	642.9287	1	642.9287	670.957	<0.0001	significant
AC	40.22344	1	40.22344	41.97697	0.0013	significant
BC	72.13804	1	72.13804	75.28288	0.0003	significant
A^2	483.8211	1	483.8211	504.9132	<0.0001	significant
B^2	680.658	1	680.658	710.331	<0.0001	significant
C^2	241.576	1	241.576	252.1074	<0.0001	significant
A^2B	455.6374	1	455.6374	475.5008	<0.0001	significant
AB^2	298.3102	1	298.3102	311.3149	<0.0001	significant
Residual	4.791132	1	0.958226	–	–	–
Lack of fit	0.084268	1	0.084268	0.071613	0.8022	not significant
Pure error	4.706864	4	1.176716	–	–	–
Cor total	7407.445	16	–	–	–	–

Table 4
ANOVA for initial rate

Source	Sum of squares	df	Mean square	*F*-value	*p*-value	
Model	1.577097	9	0.175233	74.50071	<0.0001	significant
A-pH	0.369308	1	0.369308	157.0122	<0.0001	significant
B-Fe^{2+}	0.681232	1	0.681232	289.6273	<0.0001	significant
C-H_2O_2	0.070972	1	0.070972	30.17391	0.0009	significant
AB	0.324661	1	0.324661	138.0302	<0.0001	significant
AC	0.000249	1	0.000249	0.106017	0.7542	not significant
BC	0.039398	1	0.039398	16.75003	0.0046	significant
A^2	0.022245	1	0.022245	9.457597	0.0179	significant
B^2	0.062321	1	0.062321	26.49611	0.0013	significant
C^2	0.000792	1	0.000792	0.336855	0.5798	not significant
Residual	0.016465	7	0.002352	–	–	–
Lack of Fit	0.009682	3	0.003227	1.903298	0.2704	not significant
Pure error	0.006783	4	0.001696	–	–	–
Cor total	1.593561	16	–	–	–	–

of Fe^{2+} according to Eq. (2). However, at higher pH, ACT degradation does not change significantly as [Fe^{2+}] is increased.

As seen in Fig. 5(c), increasing [H_2O_2] from 5 to 25 mmol l^{-1} always leads to an increase in ACT degradation for all combinations of pH and [Fe^{2+}] levels used in the experiments.

The amount of hydrogen peroxide added seems to dictate the oxidative power of the Fenton system as higher ACT degradation is achieved at higher hydrogen peroxide dosage. At higher H_2O_2 concentration, greater amount of oxidant is available to degrade ACT. The effects of the parameters on initial rate are summarized in Table 5. The parameter without any value

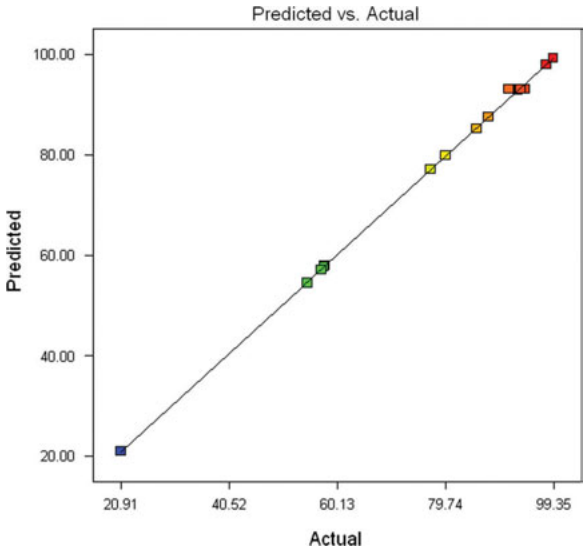

Fig. 3. Comparison of actual experimental ACT degradation with model-predicted ACT degradation.

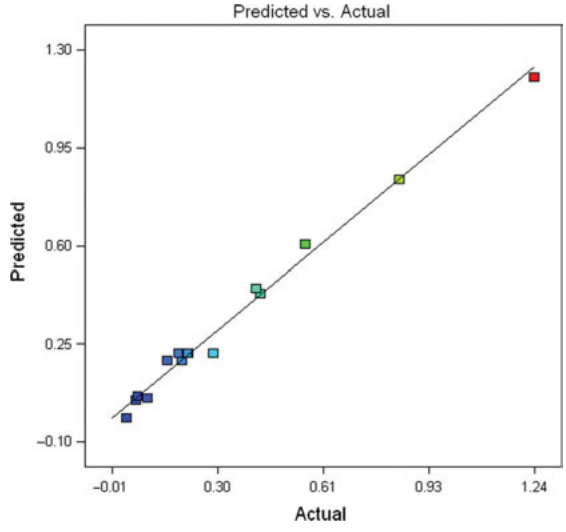

Fig. 4. Comparison of actual experimental initial rate of reaction with model-predicted initial rate.

indicated means level was varied from low level (−1) to high level (+1) while maintaining other parameters constant. Fe^{2+} concentration has the greatest effect on initial rate, increasing the rate as high as 22 times as $[Fe^{2+}]$ is increased from 0.01 to 0.1 mmol l^{-1}.

The two-parameter 3D surface plots in Fig. 6 indicate: optimum pH and Fe^{2+}dosage [Fig. 6(a)], optimum Fe^{2+} and H_2O_2 dosage [Fig. 6(b)] and optimum pH and H_2O_2 dosage [Fig. 6(c)] for maximum ACT degradation. The increase in ACT degradation resulted from the predominance of hydroxyl radical production [Eq. (1)].

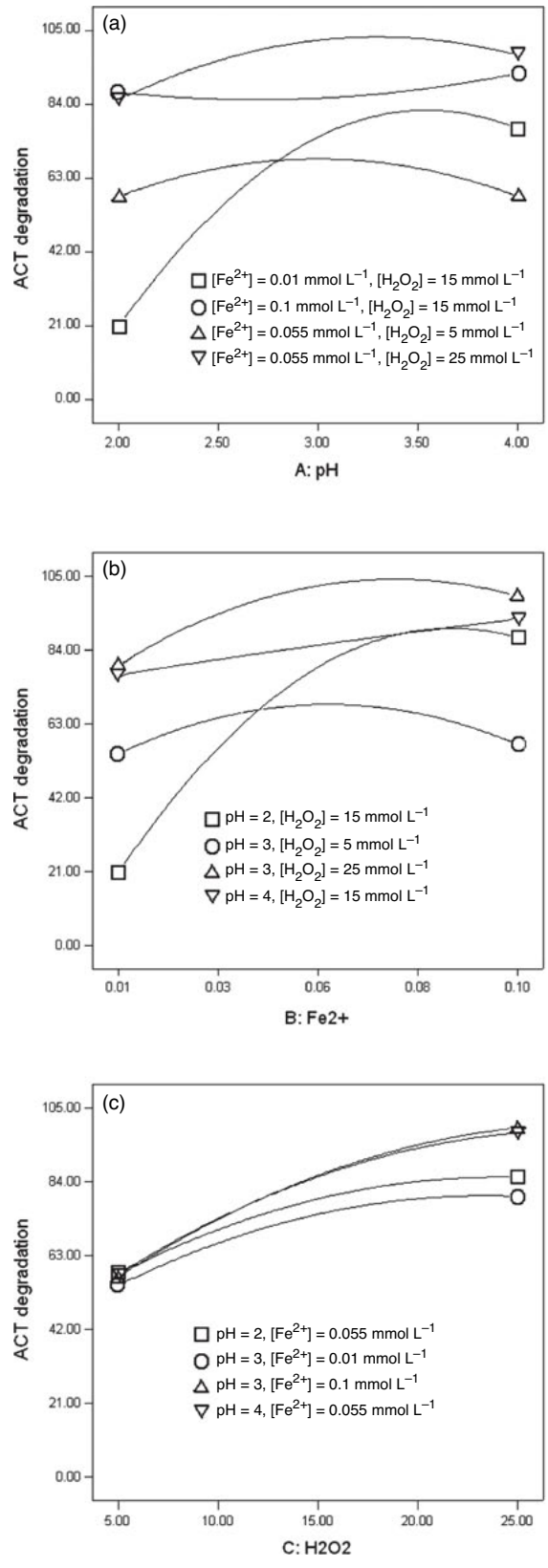

Fig. 5. Effect of (a) pH (b) $[Fe^{2+}]$ and (c) $[H_2O_2]$ on ACT degradation.

Table 5
Effect of operating parameters on the rate of ACT degradation

pH	$[Fe^{2+}]$, mM	$[H_2O_2]$, mM	$rate_{+1}/rate_{-1}$[a]
–	0.01	15	0.38
–	0.055	5	15.00
–	0.055	25	2.90
–	0.1	15	6.39
3	–	25	9.34
4	–	15	22.31
3	–	5	6.81
2	–	15	1.31
3	0.1	–	2.03
3	0.001	–	1.48
2	0.055	–	6.80
4	0.055	–	1.31

[a]$rate_{+1}$ = initial rate at high level; $rate_{-1}$ = initial rate at low level.

The observed decrease in ACT degradation can be attributed to competing reactions [Eqs. (5) and (6)] [11]. Too much H_2O_2 and Fe^{2+} in the solution would decrease the amount of oxidant (•OH).

$$H_2O_2 + \bullet OH \rightarrow H_2O + \bullet O_2H \quad k = 2.7 \times 10^7 M^{-1}s^{-1} \qquad (5)$$

$$Fe^{2+} + \bullet OH \rightarrow Fe^{3+} + OH^- \qquad (6)$$

In addition, high levels of operating parameters (pH, $[Fe^{2+}]$ and $[H_2O_2]$) promote high initial ACT degradation rates (Fig. 7).

3.2. Verification studies at optimum conditions

An appropriate solution for the reduced cubic model generated for ACT degradation is necessary for optimization. For a cost-effective operation, the amount of chemicals added was kept at a minimum while ACT degradation was set to a target of 95–100% for best degradation efficiency. The software generated only one solution with these criteria: pH = 3.22, $[Fe^{2+}]$ = 0.06 mmol l^{-1} and $[H_2O_2]$ = 19.87 mmol l^{-1}.

As shown in Table 6, the experimental results obtained for the model at optimum conditions were close to the predicted values indicating a good fit for the range of concentrations investigated.

3.3. Evaluation of fenton and fluidized-bed fenton processes at optimum conditions

Fig. 8 compares the performance of Fenton and fluidized-bed Fenton using the optimum parameters of the latter process. Both methods show similar trends

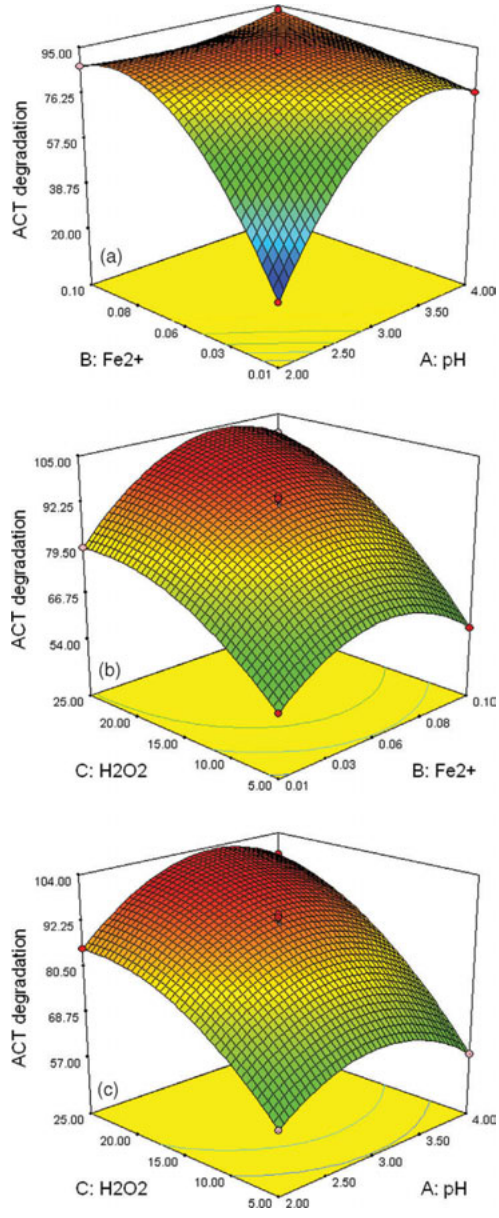

Fig. 6. 3D surface plots of the two parameter interaction effects of initial pH, $[Fe^{2+}]$ and $[H_2O_2]$ on ACT degradation: (a) $[H_2O_2]$ = 15 mmol l^{-1}, (b) pH = 3, (c) $[Fe^{2+}]$ = 0.055 mmol l^{-1}.

for most parameters (residual ACT, COD and TOC). FB-Fenton process achieved 38.2% COD removal (initial COD = 1161 mg l^{-1}) and 25.5% TOC removal (initial TOC = 596 mg l^{-1}). The marked difference between these processes lies in total residual iron.

FB-Fenton process removed 62.92% iron in solution compared to only 9.06% by the conventional Fenton process. Composition and surface area analyses of carrier material reveal transfer of iron in solution to the surface of SiO_2 particles. SEM/EDS results indicate an increase in iron content from 0.83% (Fig. 9) to 2.10% (Fig. 10)

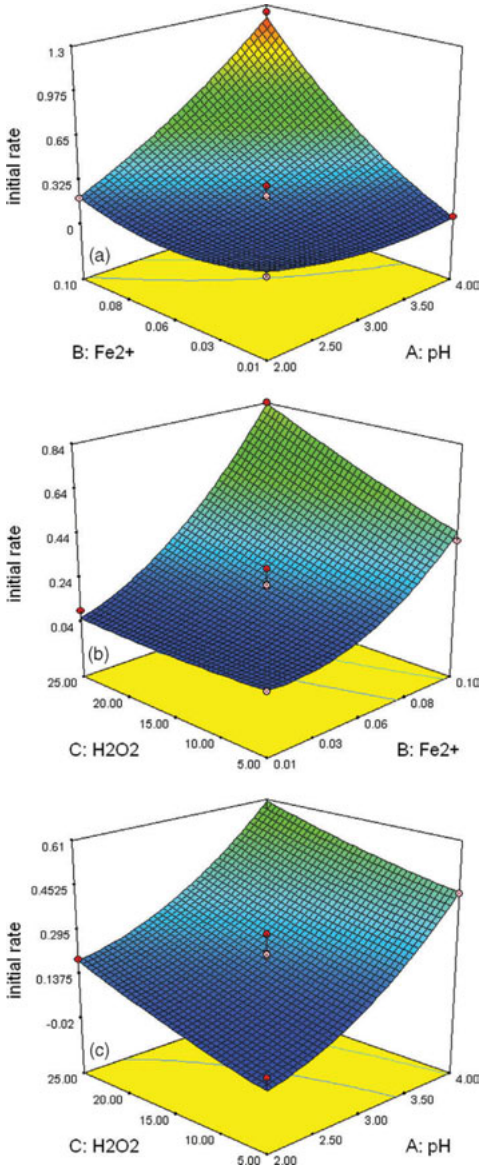

Fig. 7. 3D surface plots of the two parameter interaction effects of initial pH, [Fe^{2+}] and [H_2O_2] on initial rate: (a) [H_2O_2] = 15 mmol l^{-1}, (b) pH = 3, (c) [Fe^{2+}] = 0.055 mmol l^{-1}.

Table 6
Actual and predicted values of ACT degradation and initial rate

Response	Actual	Predicted	Difference
ACT degradation, %	97.8	100	2.2
Initial rate, mmol l^{-1} min^{-1}	0.234	0.318	0.084

while BET analysis reveals an increase in surface area from an initial of 0.154 m^2 g^{-1} to 0.314 m^2 g^{-1}. These findings confirm that SiO_2 particles served as nucleation sites for iron oxide precipitation resulting in significant reduction of iron in solution.

The performance of the optimized system in this study was further evaluated in terms of H_2O_2 efficiency as a function of COD [13], TOC [12] and ACT degradation. Hydrogen peroxide efficiency, E_H, was defined as the amount of COD [Eq. (7)], TOC [Eq. (8)] or ACT [Eq. (9)] removed (in mg) per mg O_2 available [7]. The available oxygen is the O_2 equivalent of H_2O_2 supplied, that is, 0.5 mole O_2 per mole H_2O_2 [28]:

$$E_H, \% = \frac{COD_i - COD}{(C_{Hi} - C_H) \times 0.47} \times 100\% \quad (7)$$

$$E_H, \% = \frac{TOC_i - TOC}{(C_{Hi} - C_H) \times 0.47} \times 100\% \quad (8)$$

$$E_H, \% = \frac{ACT_i - ACT}{(C_{Hi} - C_H) \times 0.47} \times 100\% \quad (9)$$

where COD_i and COD are the initial and final COD, ACT_i and ACT are the initial and final ACT concentrations, and C_{Hi} and C_H are the initial and final H_2O_2 concentrations, respectively, in mg l^{-1}. A low E_H value suggests inefficient scavenging reactions [13]. H_2O_2 efficiencies higher than 100% imply that removal is not only attributed to Fenton's reaction [7].

High hydrogen peroxide efficiencies with respect to ACT degradation and COD removal were obtained in this study (Table 7). These results suggest that the treatment process enhanced ACT oxidation. In addition, even with very little H_2O_2dosage, the process can achieve high COD removals. Low efficiency with respect to TOC removal implies that ACT was not completely mineralized to CO_2, H_2O and NH_4^+ [22].

The difference in ACT oxidation between Fenton and FB-Fenton processes was not evident at optimum conditions. However, when comparison was made at high pH (4) and low [Fe^{2+}] (0.01 mmol l^{-1}), FB-Fenton process showed better ACT degradation at 77.0% compared to only 51.7% in conventional Fenton process (Fig. 11). From the onset, initial Fe^{2+}concentration was very small and Fe^{3+} is not very soluble in aqueous solutions between pH 2 to 4. During the first 5 min of reaction, both processes had the same rate of degradation (i.e., r_{Fenton} = 0.057 mmol l^{-1} min^{-1} and $r_{FB\text{-}Fenton}$ = 0.056 mmol l^{-1} min^{-1}). At this stage, Fe^{2+} was rapidly being converted to Fe^{3+} as hydroxyl radicals were formed. However, as the reaction progressed, ACT degradation in the FB-Fenton process proceeded at a much faster rate than in the traditional Fenton process (Fig. 11). The calculated degradation rates from 5 to 20 min of reaction time were 0.099 mmol l^{-1} min^{-1} for FB-Fenton and only 0.0073 mmol l^{-1} min^{-1} for Fenton process.

For the Fenton process, Fe^{3+} are converted to Fe^{2+} but at a slower rate [Eq. (2)]. Thus, most Fe^{3+} remained

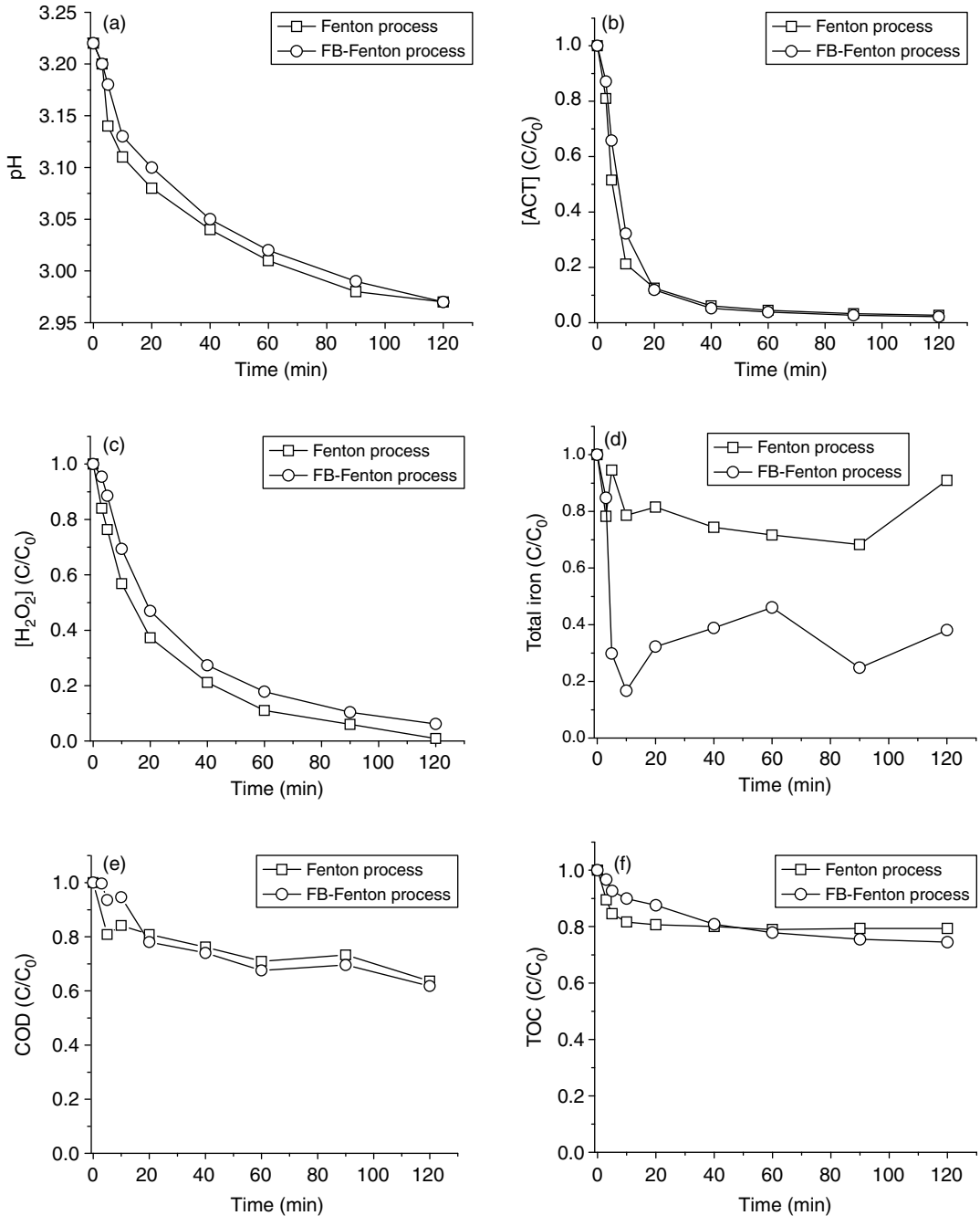

Fig. 8. Time variations of (a) pH, residual (b) ACT, (c) H_2O_2, (d) total iron, (e) COD and (f) TOC in Fenton and fluidized-bed Fenton processes at optimum conditions.

in solution as precipitates, making them incapable of catalyzing •OH production, or producing a weaker oxidant [Eq. (2)]. In contrast, the iron-coated carriers in the FB-Fenton process turned out to be heterogeneous oxidation sites for ACT degradation. At higher initial Fe^{2+} concentration, that is, at optimum conditions, the difference in ACT degradation between Fenton and FB Fenton becomes negligible as homogeneous reactions predominate over heterogeneous ones.

3.4. Comparison of FB-fenton process with other fenton-based processes

In this study, almost 95% ACT degradation was achieved after 40 min of reaction. Trovo et al. [21] studied

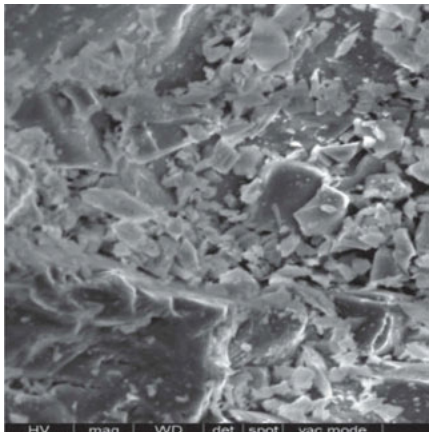

Fig. 9. Micrographs and atomic composition of SiO_2 carrier at optimum conditions before reaction.

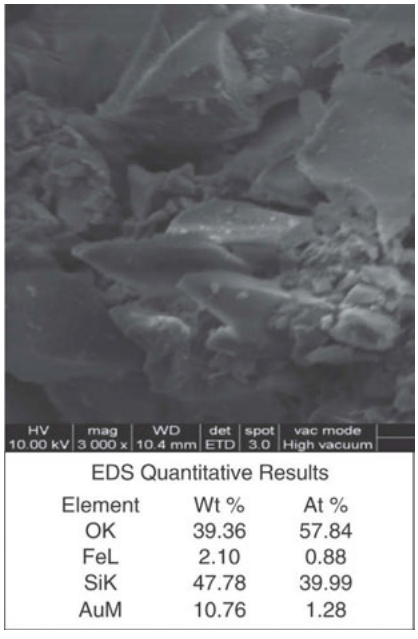

Fig. 10. Micrographs and atomic composition of SiO_2 carrier at optimum conditions after 2 h of reaction.

Table 7
H_2O_2 efficiencies of Fenton and FB-Fenton processes at optimum operating conditions

Process	E_H, %		
	COD	TOC	ACT
Fenton	137	42	201
FB-Fenton	149	50	271

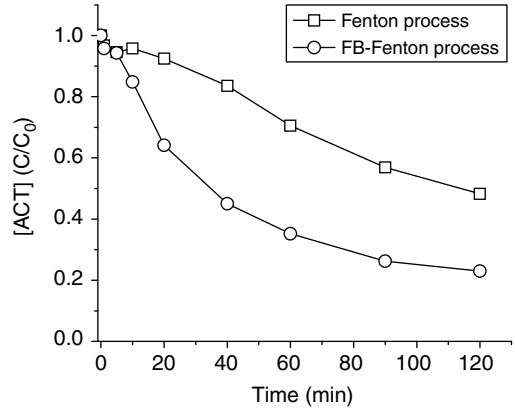

Fig. 11. ACT degradation of Fenton and fluidized-bed Fenton processes: [ACT] = 5 mmol l^{-1}, pH = 4, [Fe^{2+}] = 0.01 mmol l^{-1}, [H_2O_2] = 15 mmol l^{-1}.

photo-Fenton oxidation of ACT at lower concentration (0.1 mmol l^{-1}) using $Fe(NO)_3$ (0.20 mmol l^{-1}) as iron source. They reported 96% ACT degradation after only 10 min of irradiation at pH = 2.5 and [H_2O_2] = 5 mmol l^{-1}. Another study on the application of photo-Fenton process with continuous H_2O_2 dosage to synthetic municipal wastewater treatment plant effluent containing 0.066 mmol l^{-1} ACT was done and optimized by Duran et al. [23]. The optimum conditions were: H_2O_2 flow rate = 50 mlh^{-1}, [Fe^{2+}] = 0.036 mmol l^{-1}, pH = 2.5 and T = 40°C. At these conditions 71.5% TOC and 82.1% COD were removed in 2 h. Almeida et al. [22] applied solar photoelectro-Fenton process with in-situ H_2O_2 generation to ACT solutions (1.04 mmol l^{-1}) and also optimized the system using response surface methodology. The optimum condition was: pH = 3, [Fe^{2+}] = 0.4 mmol l^{-1} and current = 5 A, resulting in a 100% ACT degradation and 75% TOC removal after 2 h. The efficiencies of the processes with external H_2O_2 addition in terms of H_2O_2 use are shown in Table 8. Clearly, the treatment methods presented in this study are more efficient in the use of hydrogen peroxide compared to previous works.

Table 8
H_2O_2 efficiencies of Fenton-based processes for ACT degradation

Process	mol H_2O_2/mol ACT degraded	mol H_2O_2/mol TOC degraded	Reference
Fenton	4.08	1.89	this study
FB-Fenton	4.06	1.57	this study
Photo-Fenton	–	5.8	[23]
Photo-Fenton	52.08	7.79	[21]

4. Conclusions

The degradation of ACT in synthetic wastewater using fluidized-bed Fenton process was optimized in this study. From the BBD, a reduced cubic model was found to be the most suitable for ACT decomposition. All parameters, within the range of values investigated, had significant effects on ACT oxidation. By minimizing the amount of Fenton's reagents and maximizing ACT degradation, the unique solution to the model gave the optimum operating parameters at initial pH = 3.22, initial $[Fe^{2+}]$ = 0.06 mmol l^{-1} and initial $[H_2O_2]$ = 19.87 mmol l^{-1}. At these conditions, FB-Fenton caused actual ACT degradation of 97.8% in addition to significant sludge reduction removing 62.92% of total iron from the solution compared to only 9.06% by conventional Fenton process. SEM/EDS analysis confirmed that the iron taken out of the solution in the FB Fenton process coated the surface of SiO_2 carriers as iron oxides thus forming additional sites for catalytic Fenton reaction thereby enhancing ACT degradation. Moreover, the high hydrogen peroxide efficiencies of FB-Fenton process with respect to ACT decomposition and COD removal make this technology a cost-effective option in treating acetaminophen-contaminated wastewaters.

Acknowledgements

This research was financially supported by the National Science Council, Taiwan (Grant: NSC 99-2221-E-041-012-MY3) and the Department of Science and Technology, Philippines through the Engineering Research and Development for Technology (ERDT).

References

[1] K. Barbusinski, Fenton reaction-controversy concerning the chemistry, Ecol. Chem. Eng., 16 (2009) 347–358.
[2] L.A. Perez-Estrada, M.I. Maldonado, W. Gernjak, A. Aguera, A.R. Fernandez-Alba, M.M. Ballesteros and S. Malato, Decompostion of diclofenac by solar-driven photocatalysis at a pilot plant scale, Catal. Today, 101 (2005) 219–226.
[3] Y. Yavuz, EC and EF processes for the treatment of alcohol distillery wastewater, Sep. Purif. Technol., 53 (2007) 135–140.
[4] C. Mendoza-Marín, P. Osorio and N. Benítez, Decontamination of industrial wastewater from sugarcane crops by combining solar photo-fenton and biological treatments, J. Hazard. Mater., 177 (2010) 851–855.
[5] A.C. Costa Teixeira, L. Mendes, G. Stollar, R. Guardani and C.A. do Nascimento, Photo-fenton remediation of wastewaters containing agrochemicals, Braz. Arch. Biol. Technol., 48 (2005) 207–218
[6] M.-C. Lu, J.-N. Chen and C.-P. Chang, Effect of inorganic ions on the oxidation of dichlorvos insecticide with fenton's reagent, Chemosphere, 35 (1997) 2285–2293.
[7] M. Masomboon, C. Ratanatamskul and M.-C. Lu, Chemical oxidation of 2,6-dimethylaniline by electrochemically generated fenton's reagent, J. Hazard. Mater., 176 (2010) 92–98.
[8] M.-J. Liou and M.-C. Lu, Catalytic degradation of nitroaromatic explosives with Fenton's reagent, J. Mol. Catal. A: Chem., 277 (2007) 155–163.
[9] M. Skoumal, R.M. Rodríguez, P.L. Cabot, F. Centellas, J.A. Garrido, C. Arias and E. Brillas, Electro-Fenton, UVA photoelectro-fenton and solar photoelectro-fenton degradation of the drug ibuprofen in acid aqueous medium using platinum and boron-doped diamond anodes, Electrochim. Acta, 54 (2009) 2077–2085.
[10] E. Brillas, I. Sires and M.A. Oturan, Electro-fenton processes and related electrochemical technologies based on Fenton's reaction chemistry, Chem. Rev.,109 (2009) 6570–6631.
[11] W.-P. Ting, M.-C. Lu and Y.-H. Huang, Kinetics of 2,6-dimethylaniline degradation by electro-Fenton process, J. Hazard. Mater., 161 (2009) 1484–1490.
[12] J. Anotai, C.-C. Su, Y.-C. Tsai and M.-C. Lu, Effect of hydrogen peroxide on aniline oxidation by electro-Fenton and fluidized-bed Fenton processes, J. Hazard. Mater., 183 (2010) 888–893.
[13] S. Chou, C. Huang and Y.-H. Huang, Effect of Fe^{2+} on catalytic oxidation in a fluidized-bed reactor, Chemosphere, 39 (1999) 1997–2006.
[14] C. Ratanatamskul, S. Chintitanun, N. Masomboon and M.-C. Lu, Inhibitory effect of inorganic ions on nitrobenzene oxidation by fluidized-bed Fenton process, J. Mol. Catal. A: Chem., 331 (2010) 101–105.
[15] N. Boonrattanakij, M.-C. Lu and J. Anotai, Iron crystallization in a fluidized-bed Fenton process, Water Res., 45 (2011) 3255–3262.
[16] MercuryTec., Fenton Family: Advanced Oxidation Technologies for Wastewater Treatment. Retrieved October 11, 2010, from Mercury Environmental Pertection Technology: http://www.mercutec.com/pages/en/theory.html#topic2.
[17] R. Andreozzi, V. Caprio, R. Marotta and D. Vogna, Paracetamol oxidation from aqueous solutions by means of ozonation and H_2O_2/UV system, Water Res., 37 (2003) 993–1004.
[18] E. Brillas, I. Sires, C. Arias, P.-L. Cabot, F. Cantellas, R.M. Rodriguez and J.A. Garrido, Mineralization of paracetamol in aqueous medium by anodic oxidation with a boron-doped diamond electrode, Chemosphere, 58 (2005) 399–406.
[19] L. Yang, L.E. Yu and M.B. Ray, Degradation of paracetamol in aqueous solutions by TiO_2 photocatalysis, Water Res., 42 (2008) 3480–3488.
[20] X. Zhang, F. Wu, X. Wu, P. Chen and N. Deng, Photodegradation of acetaminophen in TiO_2 suspended solution, J. Hazard. Mater., 157 (2008) 300–307.
[21] A.G. Trovo, S.A.S. Melo and R.F.P. Nogueira, Photodegradation of the pharmaceuticals amoxicillin, bezafibrate and paracetamol by the photo-Fenton process—application to sewage treatment plant effluent, J. Photochem. Photobiol., A: Chem.,198 (2008) 215–220.
[22] L.C. Almeida, S. Garcia-Segura, N. Bocchi and E. Brillas, Solar photoelectro-Fenton degradation of paracetamol using a flow plant with a Pt/air-diffusion cell coupled with a compound parabolic collector: process optimization by response surface methodology, Appl. Catal., B-Environ., 103 (2011) 21–30.
[23] A. Durán, J. M. Monteagudo, A. Carnicer and M. Ruiz-Murillo, Photo-Fenton mineralization of synthetic municipal wastewater effluent containing acetaminophen in a pilot plant, Desalination, 270 (2010) 124–129.
[24] S.K. Khetan and T.J. Collins, Human pharmaceuticals in the aquatic environment: A challenge to green chemistry, Chem. Rev., 107 (2007) 2319–2364.
[25] G.E. Box and D.W. Behnken, Some new three level designs for the study of quantitative variables, Technometrics, 2 (1960) 455–475.
[26] N.-K. Nguyen and J.J. Borkowski, New 3-level response surface designs constructed from incomplete block designs, J. Stat. Plan. Infer., 138 (2008) 294–305.
[27] T.P. Davis and N.R. Draper, Fitting 3rd order terms in Box-Behnken Experiments. University of Wisconsin, Department of Statistics (1998).
[28] D.L. Pardieck, E.J. Bouwer and A.T. Stone, Hydrogen peroxide use to increase oxidant capacity for in situ bioremediation of contaminated soils and aquifers: A review, J. Contam. Hydrol., 9 (1992) 221–242.